

TOPICAL REVIEW

Red sprite discharges in the atmosphere at high altitude: the molecular physics and the similarity with laboratory discharges

V P Pasko

Communications and Space Sciences Laboratory, Department of Electrical Engineering,
The Pennsylvania State University, University Park, PA 16802, USA

E-mail: vpasko@psu.edu

Received 10 July 2006, in final form 4 December 2006

Published 31 January 2007

Online at stacks.iop.org/PSST/16/S13

Abstract

An overview of the general phenomenology and physical mechanism of large-scale electrical discharges termed ‘sprites’ observed at high altitude in the Earth’s atmosphere above thunderstorms is presented. The primary emphasis is placed on summarizing available experimental data on various emissions documented to date from sprites and interpretation of these emissions in the context of similar data obtained from laboratory discharges, in particular the pulsed corona discharges, which are believed to be the closest pressure-scaled laboratory analogue of sprite discharges at high altitude. We also review some of the recent results on modelling of laboratory and sprite streamers emphasizing the importance of the photoionization effects for the understanding of the observed morphological features of streamers at different pressures in air and provide a comparison of emissions obtained from streamer models with results of recent satellite-based observations of sprites.

(Some figures in this article are in colour only in the electronic version)

1. Introduction

The sprite phenomenon is one of four currently known forms of transient luminous events (TLEs) occurring at high altitude in the Earth’s atmosphere, which are related to the lightning activity in underlying thunderstorms ([1–3] and references cited therein). The first colour video recordings of sprites obtained during the summer of 1994 indicated that their upper portions were characterized by a bright red colour [1]. These events therefore are often referred to as ‘red sprites’ [1]. Although eyewitness reports of TLEs above thunderstorms have been recorded for more than a century, the first image of one was captured only in 1989, serendipitously during a test of a low-light television camera [4]. Since then several different types of TLEs above thunderstorms have been documented and classified and some are illustrated in figure 1.

Sprites and other TLEs are arguably the most dramatic recent discovery in solar-terrestrial physics [14]. During the

last decade several hundred papers have been published in refereed scientific literature reflecting advances in this new and exciting research area, and related research activities culminated in a first book on sprites, which appeared in print in May of 2006 [14]. The goal of this paper is to review some of the recent experimental and theoretical developments in the studies of TLEs, with emphasis on the sprite phenomenon and on the interpretation of observed optical emissions and morphological features of sprites in the context of laboratory discharges.

2. General phenomenology of sprites

Sprites are large luminous discharges, which appear in the altitude range ~ 40 – 90 km above large thunderstorms typically following intense positive cloud-to-ground lightning discharges [1, 15].

Recent telescopic imaging of sprites at standard video rates (i.e. with ~ 16 ms time resolution) revealed an amazing variety of generally vertical fine structure with transverse spatial scales ranging from tens to a few hundreds of metres [16–19]. First high-speed (1 ms) telescopic imaging of sprites has been reported indicating that streamer-like formations in sprites rarely persist for more than 1–2 ms [20, 21]. Also recently, it has been demonstrated that sprites often exhibit a sharp altitude transition between the upper diffuse and the lower highly structured regions [17, 18, 22, 23]. Many sprites are observed with an amorphous diffuse glow at their tops, the so-called sprite ‘halo’ [18,24–29].

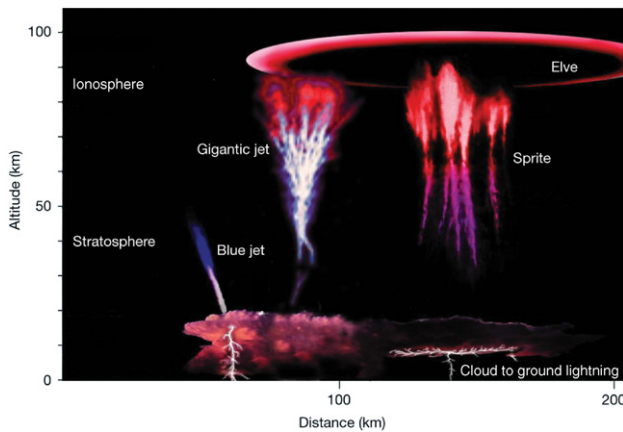


Figure 1. Lightning related TLEs. Several types of TLEs are known, and some examples are shown here: relatively slow-moving fountains of blue light, known as ‘blue jets’, which emanate from the top of thunderclouds up to an altitude of 40 km [5, 6], ‘sprites’ that develop at the base of the ionosphere and move rapidly downwards at speeds up to $10\,000\text{ km s}^{-1}$ [1, 7, 8], ‘elves’, which are lightning induced flashes that can spread over 300 km laterally [9, 10], and upward moving ‘gigantic jets’, which establish a direct path of electrical contact between thundercloud tops and the lower ionosphere [11–13]. Reprinted from [13] with permission from *Nature*.

The first continuous high-speed video recordings of sprite streamers at $\sim 10\,000$ frames/s (i.e. with $\sim 100\ \mu\text{s}$ time resolution) have recently been reported by two research groups [30–32]. Figure 2 illustrates a general scenario of development of sprites in which downward streamers appear to initiate either spontaneously or from brightening inhomogeneities at the bottom of an initially formed diffuse sprite halo and branch as they propagate downwards [30].

The appearance of fine structure in sprites (as apparent, in particular, in figure 2) has been interpreted in terms of positive and negative streamer coronas, which are considered as scaled analogues of small-scale streamers, which exist at high atmospheric pressures at ground level [23,33–36]. Streamers are filamentary plasma structures, which can initiate spark discharges in relatively short (several cm) gaps at near ground pressures in air and which are commonly utilized in applications such as ozone production and pollution control ([37, 38] and references cited therein), and also represent important components involved in the triggering of combustion in spark ignition engines [39,40]. An excellent recent review of various applications of streamers is provided in [41]. In ground air pressure applications a typical transverse scale of individual streamer filaments is a fraction of a millimetre [42, 43]. It is quite remarkable that the filamentary structures observed in sprites [19] (see also figure 2) are the same phenomenon known as streamer discharges at atmospheric pressure, only scaled by reduced air density at higher altitudes [33, 44–46]. These aspects of sprite phenomenology are important for interpretation of optical emissions observed from them and will be further discussed in subsequent sections of this paper.

3. Physical mechanism of sprites

The possibility of large-scale gas discharge events above thunderclouds, which we currently know as the sprite phenomenon, was first predicted in 1925 by the Nobel Prize winner C T R Wilson [47]. He first recognized that the relation between the thundercloud electric field which decreases with

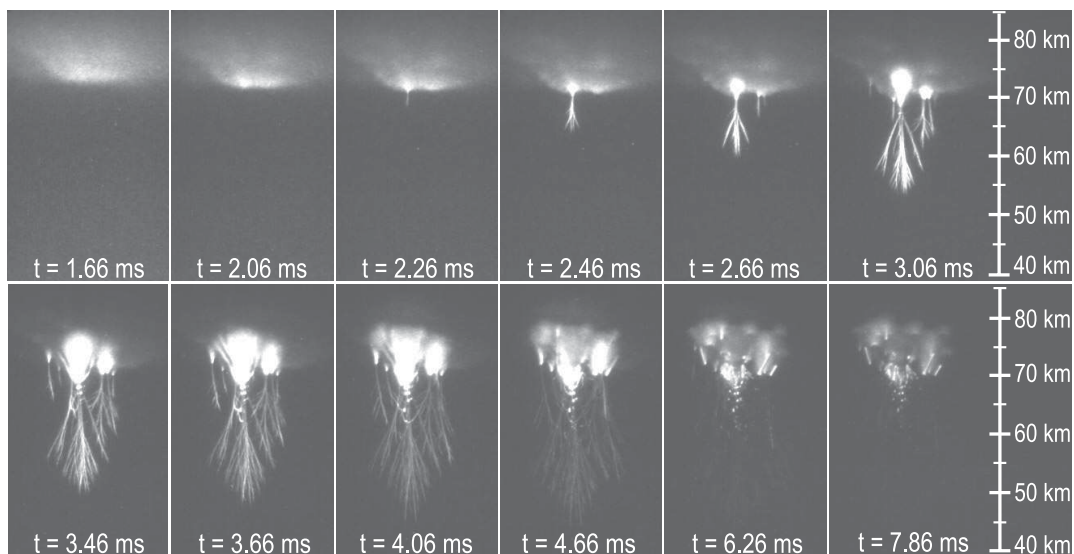


Figure 2. High-speed sprite images from 13 August 2005 at 03:12:32.0 UT, each labelled with its time from the lightning return stroke initiation [30]. Reprinted with permission from the American Geophysical Union.

altitude r (figure 3) as $\sim r^{-3}$ and the critical breakdown field E_k which falls more rapidly (being proportional to the exponentially decreasing gas density) leads to the result that ‘there will be a height above which the electric force due to the cloud exceeds the sparking limit’ [47]. Here, and in subsequent parts of this paper E_k is used to denote the conventional breakdown threshold field defined by the equality of the ionization and dissociative attachment coefficients in air [37, p 135]. It should be noted that due to the finite atmospheric conductivity above thunderclouds the dipole field configuration shown in figure 3 is realized at mesospheric altitudes only during very transient time periods $\sim 1\text{--}10$ ms following intense lightning discharges, in part defining a similarly transient nature of the observed sprite phenomenon ([48] and references cited therein).

The mechanism of the penetration of the thundercloud electric fields to the higher-altitude regions is illustrated in figure 4. As the thundercloud charges slowly build up before

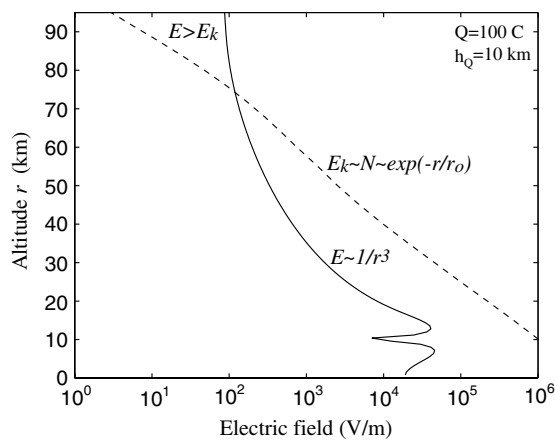


Figure 3. Physical mechanism of sprites [47]: ‘while the electric force due to the thundercloud falls off rapidly as r increase, the electric force required to cause sparking (which for a given composition of the air is proportional to its density) falls off still more rapidly. Thus, if the electric moment of a cloud is not too small, there will be a height above which the electric force due to the cloud exceeds the sparking limit.’

a lightning discharge, high-altitude regions are shielded from the quasi-electrostatic fields of the thundercloud charges by the space charge induced in the conducting atmosphere at the lower altitudes. The appearance of this shielding charge is a consequence of the finite vertical conductivity gradient of the atmosphere above the thundercloud. When one of the thundercloud charges (e.g. the positive one as shown in figure 4) is quickly removed by a lightning discharge, the remaining charges of opposite sign above the thundercloud produce a large quasi-electrostatic field that appears at all altitudes above the thundercloud and endures for a time equal to approximately (see related discussion in [48]) the local relaxation time ($\tau_\sigma = \epsilon_0/\sigma$, where σ is the local conductivity and ϵ_0 is the permittivity of free space) at each altitude. These temporarily existing electric fields lead to the heating of ambient electrons and the generation of ionization changes and optical emissions known as the sprite phenomenon.

On a conceptual level the role of the negative charge accumulating above the cloud top before the lightning discharge, as shown in figure 4, is fully analogous to a charge deposited on dielectric barriers during the quenching stage of glow discharge in miniature ac plasma display panel (PDP) cells [49]. This charge plays an important role in bringing the electric field in an ac PDP cell above the breakdown level during the voltage reversal stage of the general ac PDP firing cycle [49]. In the atmospheric case shown in figure 4 the role of dielectric barrier is played by atmospheric regions in the vicinity of thundercloud, which have much lower conductivity than those at higher altitudes. The lightning discharge plays the same role as the voltage reversal in the ac PDP cell leading to generation of large electric fields above the cloud due to charge remaining deposited on the ‘dielectric barrier’ at lower altitudes. In the case of sprites, due to the general scaling of electric field depicted in figure 3, the electric breakdown starts at high altitude, far away from the cloud top (see figure 2). In terms of general gas discharge theory [37, 45] the sprite situation corresponds to relatively large pd values, where p is the pressure and d is the effective discharge gap length, fully sufficient for development of streamers. The sprite discharges are therefore expected to proceed in the form of

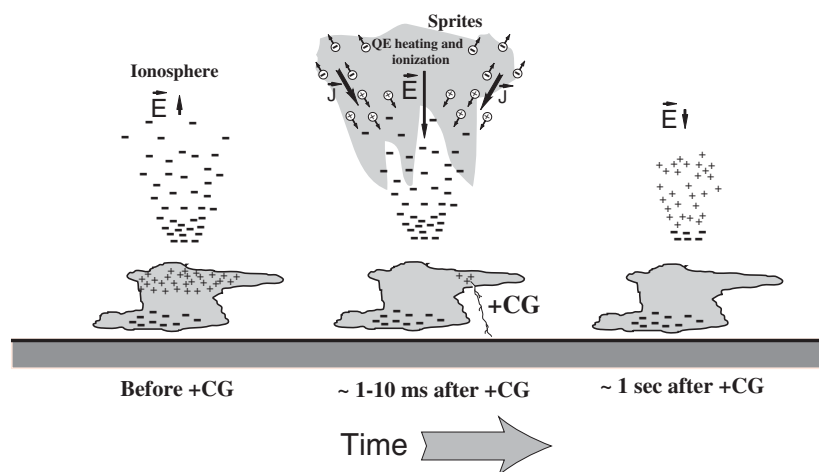


Figure 4. Illustration of the mechanism of penetration of large electric fields to mesospheric altitudes following positive cloud-to-ground (+CG) lightning discharge [48]. Reprinted with permission from the American Geophysical Union.

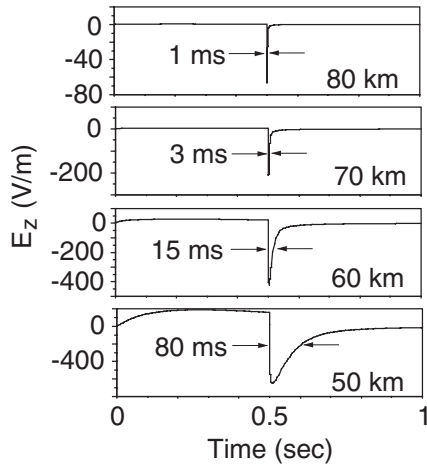


Figure 5. Time dynamics of the vertical component of the electric field at selected altitudes directly above a positive cloud-to-ground lightning discharge [48]. Reprinted with permission from the American Geophysical Union.

streamers. Some additional corrections are required to account for a relatively dense plasma at the lower ledge of the Earth's ionosphere at altitudes 80–90 km, as will be discussed further in this section.

Figure 5 illustrates the above-discussed scenario by showing model calculations of the vertical component of the electric field at altitudes 50, 60, 70 and 80 km directly above a positive lightning discharge removing 200 C of charge from the altitude 10 km in 1 ms [48]. During a very transient time period ~ 1 ms, mostly defined by the atmospheric conductivity profile, the electric field can reach values on the order of the critical breakdown threshold field E_k at mesospheric/lower ionospheric altitudes. The quasi-static approximation employed here is valid for relatively slow source variations with time scales > 0.5 ms [50].

It should be emphasized that the simplified schematics shown in figure 4 is employed to discuss the physical concept of penetration of large electric field transients to mesospheric altitudes and by no means reflects the complexity of charge distributions observed in thunderclouds. In the cases of more realistic charge distributions in the thundercloud, which sometimes involve up to six charge layers in the vertical direction [51, 52], each of the charge centres can be viewed as generating its own polarization charge in and above the thundercloud, and the resultant configuration of the electric field and charge density can be obtained by using the principle of superposition. This consideration is helpful in the visualization of the fact that the electric field appearing at mesospheric altitudes after the charge removal by cloud-to-ground lightning discharge is defined mostly by the absolute value and altitude of the removed charge and is essentially independent of the complexity of the charge configuration in the cloud. The charge removal can also be viewed as the 'placement' of an identical charge of opposite sign. The initial field above the cloud is simply the free space field due to the 'newly placed' charge and its image in the ground which is assumed to be perfectly conducting. The most recent observations indicate that most of the charge responsible for the production of sprites can be lowered from relatively low

altitudes 2–5 km, with an average height of 4.1 km for one particular storm studied in ([53] and references therein).

The charge moment change Qh_Q (i.e. charge removed by lightning Q times the altitude from which it was removed h_Q) represents the key parameter which is used in the current sprite literature to measure the strength of lightning in terms of sprite production potential [54–58]. One of the major unsolved problems in current sprite research, which is also directly evident from figure 3 depicting the field created by a charge moment $Qh_Q = 1000$ C km, is the observed initiation of sprites at altitudes 70–80 km by very weak lightning discharges with charge moment changes as small as 120 C km [55]. Several theories have been advanced to explain these observations, which include localized inhomogeneities created by small conducting particles of meteoric origin [59] and the formation of upwardly concave ionization regions near the lower ionospheric boundary associated with sprite halos [24].

In spite of the apparent simplicity of the basic mechanism of penetration of large quasi-electrostatic fields to the mesospheric altitudes described above and depicted in figure 4, the sprite morphology, sprite altitude structure and the relationship between sprite morphology and in-cloud lightning processes appear to be quite complex (see, for example, discussion in [60]).

Pasko *et al* [33] proposed a theory indicating that sprite structure as a function of altitude should exhibit a transition from essentially nonstructured diffuse glow at altitudes ≥ 85 km to the highly structured streamer region at altitudes ≤ 75 km (figure 6). It is proposed that the vertical structuring in sprites is created due to an interplay of three physical time scales: (1) the dissociative attachment time scale τ_a (which is defined by the maximum net attachment frequency as $1/(v_a - v_i)_{\max}$, where v_i and v_a are the ionization and attachment frequencies, respectively); (2) the ambient dielectric relaxation time scale $\tau_\sigma = \epsilon_0/\sigma$; (3) the time scale for the development of an individual electron avalanche into a streamer t_s (this is an effective time over which the electron avalanche generates a space-charge field comparable in magnitude to the externally applied field [33]). The interplay between these three parameters creates three unique altitude regions as illustrated in figure 6: (1) the diffuse region ($\tau_\sigma < \tau_a$, $\tau_\sigma < t_s$) characterized by simple volumetric multiplication of electrons (Townsend electron multiplication mechanism); (2) the transition region ($\tau_\sigma > \tau_a$, $\tau_\sigma < \sim t_s$) characterized by strong attachment of ambient electrons before the onset of the electrical breakdown; (3) the streamer region ($\tau_\sigma > \tau_a$, $\tau_\sigma > t_s$) also characterized by the strong attachment as well as by individual electron avalanches evolving into streamers. The upper and lower boundaries of the transition region shown in figure 6 represent an estimate of the altitude range in which the actual transition between the diffuse and streamer regions is expected to occur. The upper boundary may shift downwards under conditions of an impulsive lightning discharge which generates substantial electron density (i.e. conductivity) enhancement associated with the sprite halo at the initial stage of sprite formation [24]. The lower boundary may shift upwards due to streamers originating at lower altitudes but propagating upwards towards the lower ionosphere [8].

Barrington-Leigh *et al* [24] conducted a one-to-one comparison between high-speed video observations of sprites

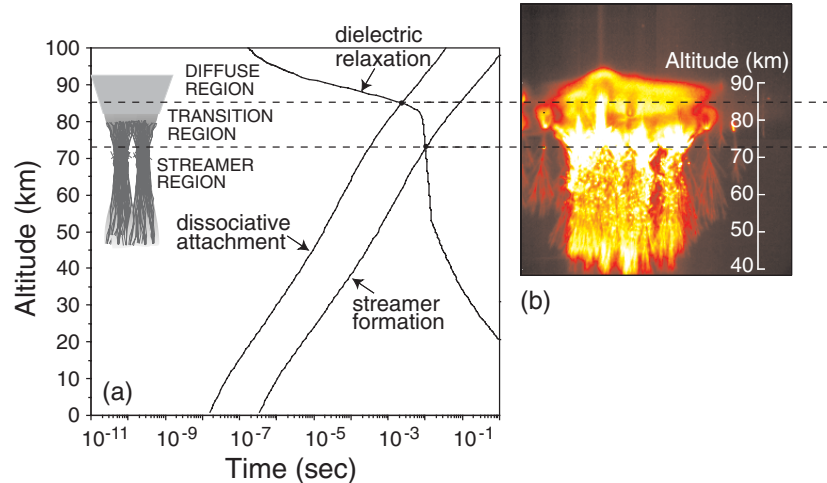


Figure 6. The vertical altitude structuring of optical emissions in sprites. (a) The altitude distribution of different time scales characterizing the vertical structuring of optical emissions in sprites [33,23]. (b) Results of video observations [22]. Reprinted with permission from the American Geophysical Union.

Table 1. Summary of emissions from sprites [62].

Emission band system	Transition	Excitation energy threshold (eV)	Lifetime at 70 km Alt.	Quenching Alt. (km)
1PN ₂	N ₂ (B ³ Π _g)→N ₂ (A ³ Σ _u ⁺)	~7.35	5.4 μs	~53
2PN ₂	N ₂ (C ³ Π _u)→N ₂ (B ³ Π _g)	~ 11	50 ns	~30
LBH N ₂	N ₂ (a ¹ Π _g)→N ₂ (X ¹ Σ _g ⁺)	~8.55	14 μs	~77
1NN ₂ ⁺	N ₂ ⁺ (B ² Σ _u ⁺)→N ₂ ⁺ (X ² Σ _g ⁺)	~18.8	69 ns	~48

and a fully electromagnetic model of sprite driving fields and optical emissions. Sprite halos are brief descending glows with lateral extent 40–70 km, which are sometimes observed to accompany or precede more structured sprites. The analysis conducted in [24] demonstrated very close agreement between model optical emissions and high-speed video observations and for the first time identified sprite halos as being produced entirely by quasi-electrostatic thundercloud fields. Sprites indeed often exhibit sprite halos, which appear as relatively amorphous non-structured glow at sprite tops and which convert to highly structured regions at lower altitudes ([8,16] and references therein). This vertical structure in sprites is apparent in recent high-speed video images of Stenbaek-Nielsen *et al* [22], was reported during telescopic observations of sprites by Gerken and Inan [17] and during recent satellite observations [61] and can be clearly seen in figures 2 and 6(b).

4. Observations of emissions associated with sprites

Table 1 [62] summarizes emissions documented in sprites. These include the first positive (1PN₂) and second positive (2PN₂) band systems of N₂, N₂ Lyman–Birge–Hopfield (LBH) band system and the first negative band system of N₂⁺ (1NN₂⁺). In this section we provide a review of related observations.

Spectra of sprites in the stratosphere/mesosphere above electrically active cumulonimbus clouds were acquired on 16 July 1995, from an observation site near Fort Collins, Colorado, by Mende *et al* [63]. The observations were conducted with a spectral resolution approximately 9 nm and spectra recorded at a normal video rate (33 ms/frame) using an

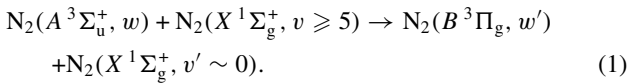
imaging spectrometer [63]. The spectra, resolved from ~450–800 nm, included four distinct features in the 600–760 nm region which have been identified as the N₂ first positive system with $\Delta = 2, 3$ and 4 from the $v = 2, 4, 5, 6$ vibrational levels of the B³Π_g state.

Hampton *et al* [64] used a video slit spectrograph to obtain optical spectra of sprites. Twenty five events were observed from the Mount Evans Observatory over a thunderstorm on the border of Nebraska and Colorado between 0700 and 0900 UT on the night of 22 June 1995. For 10 of these events optical spectra were measured in the wavelength range 540–840 nm with spectral resolution approximately 6 nm and recorded with a 33 ms time resolution. After correcting for the spectrograph response function, digitized spectrograph video images were used to measure the wavelength of, and the ratios between, the various emissions. All emissions were found to be those of the first positive band system of N₂.

The first spectrally resolved emissions obtained in [63,64] have been analysed in detail by Green *et al* [65] using energy dependent electron excitation cross sections and laboratory data to extract information on the vibrational distributions of the excited N₂ B³Π_g state and the energies of electrons producing the red sprite radiance. It has been concluded that the sprite electrons appear to be of energy sufficient to dissociate and ionize N₂. Results indicated excitation by electrons with a Boltzmann temperature of 1 eV (range 0.4–2 eV) [65]. Green *et al* [65] also derived an estimate for the electric field magnitude driving sprite phenomenon of 100–200 V m⁻¹ at 70 km altitude. This field appears to be fully consistent with the breakdown field E_k depicted in figure 3.

The spectral resolution (6–9 nm) employed in [63, 64] has not permitted accurate rotational temperature determination [65], and we note that up to the present date there are no data available on the rotational temperature in sprites. In existing sprite models the rotational lines are computed at a temperature 220–230 K [65, 66]. Recently, well-distinguishable infra-sound signatures of sprite events have been reported [67–69], indicating a possibility of heating of ambient atmospheric gas by sprite discharges. The measurements of rotational intensity distributions of N_2 molecular bands may be potentially used for remote sensing of variations of gas temperature in sprite discharges [70, 71, p 157].

A time-dependent N_2 vibrational level population model has been used in [72] to simulate the spectral distributions and absolute intensities observed in sprites. Comparison of modelling results with the sprite spectrum taken at the TV field rate (17 ms resolution) measured with 7–11 nm resolution from the Wyoming Infrared Observatory (WORO) on Jelm Mountain during July 1996 led to a vibrational distribution of the $N_2(B^3\Pi_g)$, which required an average electron energy of only 1–2 eV, generally consistent with earlier results reported in [65]. Analysis also indicated the presence of spectral features, which are attributable to N_2^+ Meinel emission [72]. Additional analysis of a sprite spectrum from 53 km altitude from the same data set has been conducted in [66]. The obtained $N_2(B^3\Pi_g)$ vibrational distribution appeared to be consistent with those observed in laboratory afterglows, indicating an energy transfer process at lower altitudes in sprites (i.e. in sprite tendrils) between vibrationally excited N_2 ground state and the lowest-energy, metastable electronic state:



The recently reported altitude-resolved sprite spectra [73, 74] recorded with an imaging spectrograph with 3 ms and 3 nm temporal and spectral resolution, respectively, are consistent with this hypothesis. The metastable oxygen molecules $O_2(a^1\Delta_g)$ are abundantly produced in streamer discharges [75, 76], and a possible contribution to sprite $N_2(B^3\Pi_g)$ emissions of energy transfer between $O_2(a^1\Delta_g)$ and $N_2(A^3\Sigma_u^+)$ metastable species has recently been discussed in [77].

The low temporal resolution (~ 17 – 33 ms) of spectral measurements in [63, 64], and in the spectra used for subsequent analysis reported in [65, 66, 72], represents a likely reason why more energetic electrons and higher electric fields, associated with streamer tips, have not been detected in these early measurements. A sub-millisecond time resolution is needed for accurate studies of sprite streamers (see figure 2, for example). Following original observations of [63, 64], narrow band photometric and blue-light video observations of sprites had been conducted [78–80], which indicated presence of a short (< 1 ms) energetic ionizing event at the initial stage of sprite formation sufficient to ionize and excite molecular nitrogen, followed by secondary lower energy processes which give rise to the dominant and relatively long-lasting red emission. Specifically, sub-millisecond time resolution data on the 399.8 nm $N_2(1,4)$ second positive band, 427.8 nm $N_2^+(0,1)$ and 470.9 nm $N_2^+(0,1)$ first negative bands generated by

sprites have been obtained and analysed for the first time in conjunction with supporting video imaging in [78–80]. The measured impulsive ionization emission during the sprite initiation exhibited an exponential decay time constant of only 0.3 ms. The presence of more energetic electrons at the initial stage of sprite formation has also been confirmed by subsequent photometric observations reported in [27, 81].

During the EXL98 aircraft mission, sprites were observed by narrow band cameras that measure the N_2^+ first negative (0,1) band at 427.8 nm and the N_2 second positive (0,0) band at 337.0 nm [82]. The observations integrated the sprite emissions over 33 ms so that temporal information was limited. The analysis indicated characteristic electron energies on the order of 2 eV and the electric field magnitudes which closely followed the breakdown field E_k up to 55 km altitude and dropped below E_k above 55 km [82]. These results are generally consistent with previous observations reviewed above conducted with similar time resolution.

The recently launched FORMOSAT-2 satellite carries the Imager for Sprites and Upper Atmospheric Lightning (ISUAL) instrument [83–86]. The ISUAL science payload provides a unique opportunity to conduct global survey of sprites and other TLEs from space using an intensified CCD imager, a six channel spectrophotometer and two array photometers [85], avoiding many complications, which usually arise during observations from ground-based and airborne platforms due to atmospheric transmission effects in the blue, violet and ultraviolet regions of the spectrum. Recently, in addition to the high time resolution photometric data on $1PN_2$, $2PN_2$ and $1NN_2^+$ sprite emissions, the ISUAL instrument has successfully observed far-UV (FUV) emissions from sprites due to the N_2 Lyman–Birge–Hopfield (LBH) band system [84–86]. An example of interpretation of recent sprite data obtained by the ISUAL instrument in the context of theory of sprite streamers will be presented in section 6.

5. Comparison of sprite emissions with emissions from laboratory discharges

In this section we compare the emissions observed in sprites reviewed in previous section with a selected set of spectroscopic measurements of pulsed corona discharges in laboratory experiments. We note that principal approaches to remote sensing of electron energy distributions in sprites using absolute intensities and ratios of various emission bands arising from excited electronic states of neutral and ionized molecular nitrogen have been extensively discussed in the existing sprite literature [27, 62, 79, 81–84, 87–89]. In particular, figure 7 illustrates the distribution of excitation frequencies for several electronic states of N_2 and N_2^+ of interest in sprite studies (see table 1) as a function of reduced electric field, which were used in recent modelling studies of sprite streamers [44, 62, 88, 90]. The ratios of various emissions arising from these states are very sensitive functions of the driving electric field and, if measured experimentally, can be directly compared with optical emission models such as those used in [44, 62, 88] (accounting for excitation and photon emission as well as quenching and cascading effects) to extract information about effective driving electric fields and consequently electron energy distributions responsible for these emissions. These

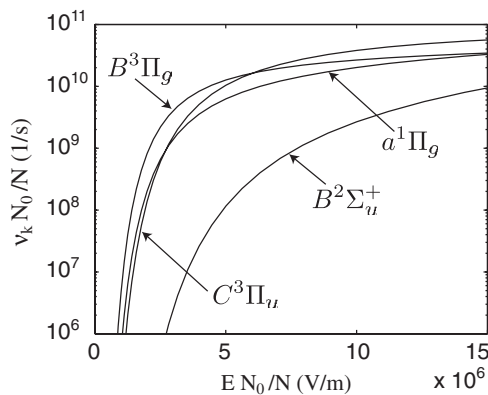


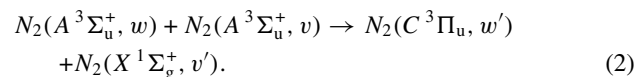
Figure 7. The excitation frequencies ν_k of the $B^3\Pi_g$, $C^3\Pi_u$ and $a^1\Pi_g$ states of N_2 and the $B^2\Sigma_u^+$ state of N_2^+ as a function of reduced electric field in air [88, 90]. See also <http://pasko.ee.psu.edu/air>. Reprinted with permission from the American Geophysical Union.

approaches are generally similar to those used in spectroscopic studies of laboratory streamers. The main intent of the rest of this section is to emphasize certain features of emissions observed in laboratory discharges which can be potentially useful for a better understanding of sprite phenomenology.

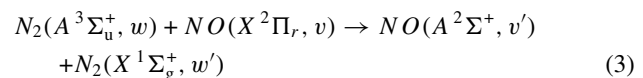
Gallimberti *et al* [91] discussed general approaches for deriving mean energies of electrons in impulse corona discharges in air at atmospheric pressure using ratios of intensities of various bands belonging to the N_2 second positive and N_2^+ first negative band systems. The results were normalized by intensity of the (0,2) band of the N_2 second positive system and it was noted that the relative intensities of the bands within the N_2 second positive system could be used to derive information about energy of electrons driving the discharge only for relatively low electron energies, as the ratios become insensitive to the mean electron energy above ~ 5 – 6 eV for both Druyvesteyn and Maxwellian electron energy distributions studied in [91]. This result is consistent with findings in [92, 93] indicating that the vibrational excitation of the $N_2 C^3\Pi_u$ state by electron impact increases with electron temperature T_e in the range 1–5 eV, but becomes weakly sensitive at $T_e > 5$ eV. The ratios of first negative bands of N_2^+ to the (0,2) band of the N_2 second positive system discussed in [91] exhibited a much steeper variation as a function of mean electron energy and therefore provided a more reliable assessment of the electron energy distribution. The direct inspection of the sharp difference among excitation frequencies of $N_2(C^3\Pi_u)$ and $N_2^+(B^2\Sigma_u^+)$ electronic states as a function of the reduced electric field shown in figure 7 further supports essentially the same point by indicating that ratios of emissions arising from these states can be used for the accurate measurement of driving electric field. These results illustrate a basic reason why the ratios of intensities of emissions from states with markedly different energy excitation thresholds such as those of $N_2(C^3\Pi_u)$ and $N_2^+(B^2\Sigma_u^+)$ (see table 1 and figure 7) are widely used in spectroscopic studies of pulsed corona discharges ([91, 93–97] and references therein). The ratios of emission intensities produced by the 0–0 transitions of the second positive system of N_2 and the first negative system of N_2^+ have also been used recently for spatio-temporal diagnostics of the filamentary and diffuse mode of the barrier discharges in air at atmospheric pressure [98, 99]. Essentially

the same approaches have been adopted in recent years to the studies of sprite discharges [27, 61, 62, 79, 81–84, 87–89]. The $N_2(C^3\Pi_u)$ and $N_2^+(B^2\Sigma_u^+)$ states have certain advantages in the case of studies of electron energy distributions at early stages of non-thermal streamer discharges as they are predominantly produced by direct electron impact of the ground state N_2 molecule (i.e. they are not contaminated by cascading and energy transfer effects) [95, 96]. We note that the $N_2(B^3\Pi_g)$ state playing an important role in sprite emissions is heavily quenched in laboratory experiments conducted at near ground pressures (see table 1 and [94]).

It is believed that pulsed positive corona discharges in N_2 – O_2 mixtures used for generation of non-equilibrium plasma at atmospheric pressure for environmental applications [92, 100–102] represent a closest laboratory analogue of sprite streamers formed under impulsive application of lightning-related quasi-static electric fields as described in section 3 and illustrated in figures 4 and 5. The time-resolved spectroscopic studies of pulsed positive corona discharges indicate the presence of two distinct phases of the discharge development: the initial phase, associated with propagation of streamers and direct excitation of ground state nitrogen molecules by electron impact, and the post-discharge phase, during which emissions from the discharge are controlled by $N_2(A^3\Sigma_u^+)$ metastable species via energy pooling and resonant energy transfer processes [92, 100–102]. During the initial phase most of the $N_2(C^3\Pi_u)$ emission comes from the high field regions around heads of streamers [92, 100], while during the post-discharge period the $N_2(C^3\Pi_u)$ formation is dominated by the energy pooling reaction [92]:



The atomic oxygen formed as a result of dissociation of oxygen molecules by electron impact during the initial phase can interact with $N_2(A^3\Sigma_u^+)$ metastables leading to the formation of $NO(X^2\Pi_r)$ species [92]. The $NO(X^2\Pi_r)$ species are also effectively formed due to fast interaction of molecular oxygen with excited $N(^2D)$ atoms formed as a result of electron impact dissociation of N_2 [103–106]. The resonant transfer reaction



is well established to be the source of NO γ -band emission radiated via $NO(A^2\Sigma^+) \rightarrow NO(X^2\Pi)$ [92, 101, 102, 107]. For these reasons the NO- γ emission is frequently used to monitor the evolution of $N_2(A^3\Sigma_u^+)$ species [92, 101, 102]. The NO- γ is expected to be produced in sprite discharges as well, following exactly the same excitation mechanisms. We note that NO- γ emissions generally appear in the same FUV range of wavelengths as LBH N_2 emissions [101] and therefore may have contributed to sprite emissions recently detected in the 150–280 nm wavelength range by the ISUAL spectrophotometer on FORMOSAT-2 satellite [84–86]. It is noted that the rotational structure of $NO(A^2\Sigma^+)$ is strongly influenced by the reaction process (3) and therefore NO- γ emission does not represent a good measure for gas temperature estimation [92, 101, 107].

6. Modelling of sprite streamers and comparison with recent satellite observations and laboratory experiments

Streamers are needle-shaped filaments of ionization embedded in originally cold (near room temperature) air and driven by strong fields due to charge separation in their heads [37, p 334]. The streamer polarity is defined by a sign of the charge in its head. The positive streamer propagates against the direction of the electron drift and requires ambient seed electrons avalanching towards the streamer head for the spatial advancement [108]. The negative streamer is generally able to propagate without the seed electrons since electron avalanches originating from the streamer head propagate in the same direction as the streamer [109, 110]. A detailed review of various properties of streamers, including fields required for their initiation and propagation, and similarity relationships allowing scaling of streamer parameters as a function of gas pressure for the purposes of interpretation of sprite discharges, is provided in [45].

Significant progress has been achieved in recent years in high spatial [19] and temporal [30] resolution imaging of streamers at low air pressures in transient luminous events in the Earth's atmosphere, as well as in relatively small discharge volumes in laboratory experiments at near ground air pressures [42, 43]. Understanding of similarities and dissimilarities of streamers at different pressures observed in these experiments represents an important problem, resolution of which would synergistically benefit the understanding of streamers in both systems (i.e. due to generally relaxed requirements on the time resolution of imaging systems needed for studies of streamers at low air pressures in transient luminous events and easy repeatability of discharges in high pressure laboratory experiments).

Similarity relations ([111, 46] and references therein) represent a useful tool for analysis of gas discharges since they allow us to use known properties of the discharge at one pressure to deduce features of discharges at a variety of other pressures of interest, at which experimental studies may not be feasible or even possible. Similarity laws for streamers propagating in non-uniform gaps in air at high (i.e. several atmospheric) pressures have been studied in [39, 112]. The similarity properties of streamers at different air pressures are also of great interest for the interpretation of morphology observed in high-altitude sprite discharges [33, 44].

It is well established by now that the dynamical properties and geometry of both positive and negative streamers can be affected by the population of the ambient seed electrons, and many of the recent modelling studies have been devoted to understanding the role of the ambient medium pre-ionization, including the effects of photoionization by UV photons originating from a region of high electric field in the streamer head, on the dynamics of negative [110, 113] and positive [113–115] streamers in different mixtures of molecular nitrogen (N_2) and oxygen (O_2) gases and in air at ground pressure.

The importance of the photoionization effects on sprite streamers at low air pressures at high altitudes is underscored by the fact that the effective quenching altitude of the excited N_2 states $b^1\Pi_u$, $b^1\Sigma_u^+$ and $c^1\Sigma_u^+$ that give the photoionizing radiation is about 24 km (corresponding to the air pressure

$p = p_q = 30$ Torr) [116]. The quenching of these states is therefore negligible at typical sprite altitudes 40–90 km, leading to an enhancement of the electron–ion pair production ahead of the streamer tip due to the photoionization, when compared with the previous studies of streamers at ground level. This and other effects have recently been studied by Liu and Pasko [44] using a newly developed streamer model and some principal results of these studies will be outlined below. The recent discussion of the validity of the photoionization model of Zheleznyak *et al* [116], that is widely used for streamer simulations and is adopted in the model reported in [44], can be found in [117, 118]. It is noted that fast electron detachment in an electric field could be an effective source of seed electrons for repetitively pulsed discharges in electronegative gases [117]. The work by Naidis [118] emphasizes the importance of accounting for the quenching of radiating states and absorption of photoionizing radiation by water molecules for the correct interpretation of recent experimental data on ionizing radiation in discharges in dry and humid air. A new computationally efficient approach to the calculation of the photoionization source in streamer models based on an approximate radiative transfer equation has recently been proposed in [119].

6.1. Dynamical properties of streamers in strong uniform electric fields

The strong and weak field model cases discussed in this and subsequent subsections refer to applied electric field magnitudes E_0 above and below the conventional breakdown threshold field E_k , respectively.

Figure 8 illustrates results of model calculations of electron densities corresponding to double-headed streamers developing at altitudes 0, 30 and 70 km in electric field $E_0 = 1.5E_k$. In accordance with the similarity relationships, the streamer time scales the streamer spatial scales, and the streamer electron densities scale with the air density as $\sim 1/N$, $\sim 1/N$ and $\sim N^2$, respectively, and the scaled streamer characteristics remain otherwise identical for the same values of the reduced electric field E/N [33]. In order to facilitate discussion of similarity properties of streamers at different altitudes/air densities, the results presented in figures 8(b) and (c) are given at the moments of time, which are obtained by scaling ($\sim 1/N$) of the ground value, 2.7 ns, specified in figure 8(a). The horizontal and vertical dimensions of the simulation boxes in figures 8(b) and (c) also directly correspond to scaled ($\sim 1/N$) ground values shown in figure 8(a). The electron density scale in figures 8(b) and (c) also corresponds to scaled ($\sim N^2$) values given in figure 8(a). The differences observed between model streamers at the ground and at 30 and 70 km altitudes in figure 8 are primarily due to the reduction in photoelectron production at high atmospheric pressures through the quenching of UV emitting excited states of N_2 [44]. In all the cases shown model streamers exhibit fast acceleration and expansion [44].

The fast expansion and acceleration are important characteristics of the considered model streamers. For instance, a positive streamer initiated in the $1.1E_k$ field at 70 km altitude would reach an effective diameter of 110 m and speed of about one-tenth of the speed of light (2.2×10^7 m s⁻¹)

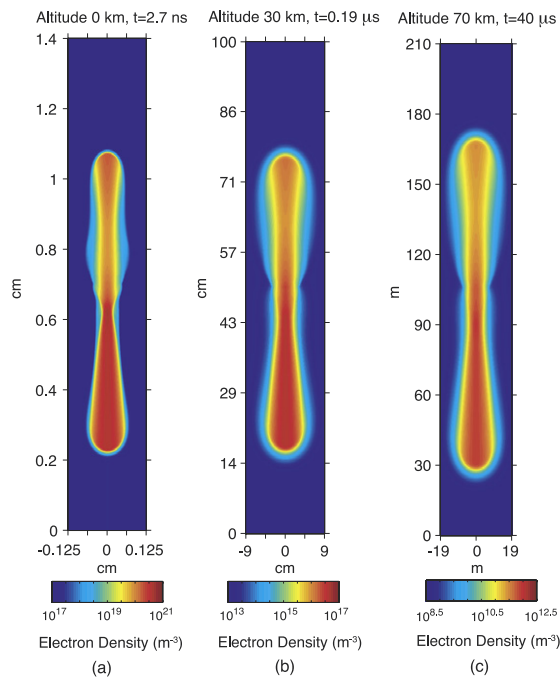


Figure 8. A cross-sectional view of the distribution of the electron number density of the model streamers at altitudes (a) 0 km, (b) 30 km and (c) 70 km [44]. Reprinted with permission from the American Geophysical Union.

by travelling a distance of only 1 km [44]. Such high speeds of sprite streamers indeed have been recently documented by high-speed video [8, 28, 120] and multi-channel photometric [121] systems. The initiation of sprites at altitudes 70–75 km in a form of simultaneous upward and downward propagating streamers is also well documented [8, 22, 28, 120, 121]. It is clear, however, that the effective streamer diameters observed by an imager zooming on sprite structures at different altitudes would inevitably depend on the geometry of the mesospheric electric fields and the history of the sprite development (i.e. the altitude of the initiation point(s)). Gerken *et al* [16] and Gerken and Inan [17, 18] have recently employed a novel telescoping imager to measure effective streamer diameters at different altitudes in sprites. The measured diameters are 60–145 m (± 12 m), 150 m (± 13 m), 196 m (± 13 m) for altitude ranges 60–64 km (± 4.5 km), 76–80 km (± 5 km), 81–85 km (± 6 km), respectively. Although the 60–145 m (± 12 m) is more than one order of magnitude greater than the scaled initial diameters of streamers shown in figure 8(c) (at 60 km, $2r_s \simeq 4$ m), given the realistic charge moments available for the sprite initiation [55], it is likely that streamers appearing at these low altitudes were initiated at much higher altitudes and propagated long distances experiencing substantial expansion. All observed diameters by Gerken *et al* [16] and Gerken and Inan [17, 18] can therefore be realistically accounted for by the modelling studies presented in [44].

We emphasize that the ~ 100 μ s time resolution, which is needed for studies of dynamic properties of streamers in sprites (i.e. streamers shown in figure 8(c)), has recently been achieved by two research groups, which performed first continuous high-speed video recordings of sprite streamers at ~ 10000 frames/s [30–32]. As was pointed above, the studies of streamers in sprites at low air pressures and their similarity

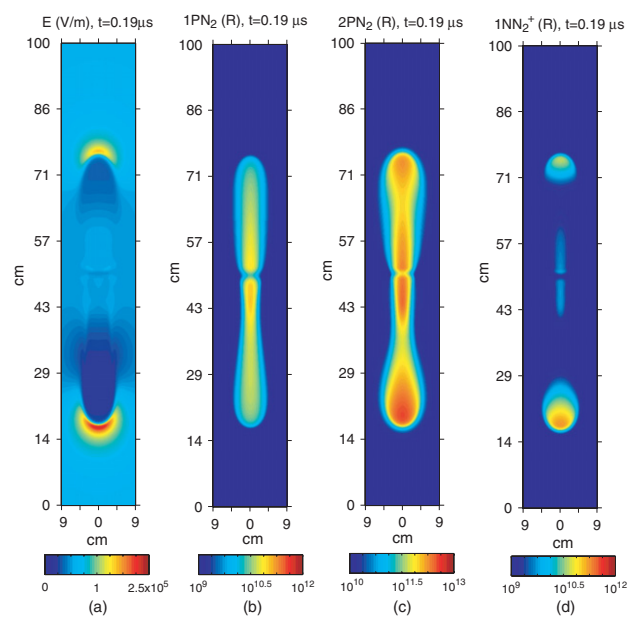


Figure 9. The magnitude of the electric field (a) and the intensity of optical emissions (in Rayleighs) in selected band systems (b)–(d) associated with the model streamers at altitude 30 km [44]. Reprinted by permission from the American Geophysical Union.

properties, in particular, represent an area of research, which may synergistically benefit the understanding of streamers used in high (i.e. near ground) pressure applications, which require sub-nanosecond time resolution for continuous video imaging (see time scales, for example, in figure 8(a), and discussion in [122]).

6.2. Optical emissions from streamers in strong uniform electric fields

Figures 9 and 10 illustrate distributions of the electric field magnitude and intensities of optical emissions (in Rayleighs) corresponding to the model streamers at 30 km and 70 km altitudes, respectively, at the same instants of time as specified in figure 8. The strong blue emissions (associated with 1st negative N₂⁺ (1NN₂⁺) and 2nd positive N₂ (2PN₂) band systems, figures 10(c) and (d)), originating primarily in the streamer heads are expected to be produced during the early time of sprite development, as the sprite develops over its altitude extent on a short time scale with respect to the total sprite emission time. This agrees well with recent narrow band photometric and blue-light video observations of sprites [78–80, 82] indicating short duration (\sim ms) bursts of blue optical emissions appearing at the initial stage of sprite formation. It is believed that this stage of sprite development is directly analogous to the initial phase of the pulsed positive corona discharges discussed in section 5. The time-averaged optical emissions are expected to be dominated by red emissions associated with the first positive band system of N₂ (1PN₂, figure 10(b)), which has the lowest-energy excitation threshold (~ 7.35 eV) and can be effectively produced by relatively low electric fields in the streamer channels, in agreement with sprite observations [63, 64, 66, 72, 81, 82]. Referring to table 1 we also note that the suppression of 1PN₂ emissions due to the strong quenching of the N₂ B³P_g state

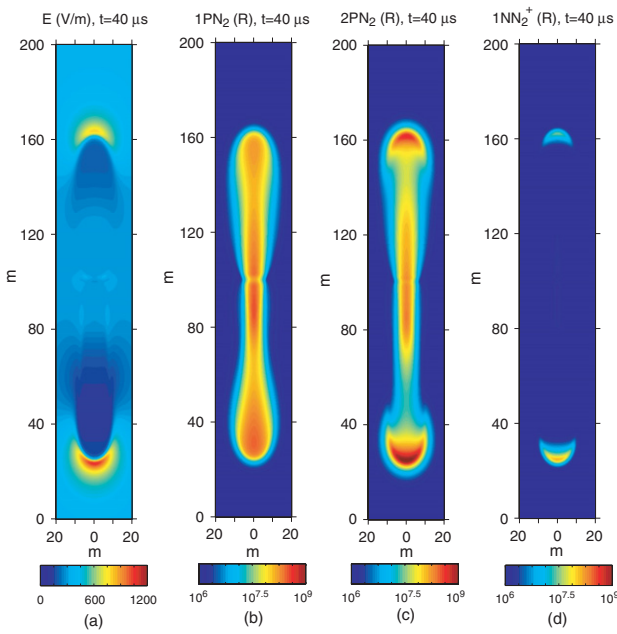


Figure 10. The same as for figure 9 only for model streamers at an altitude of 70 km [44]. Reprinted with permission from the American Geophysical Union.

at altitudes below 50 km [71, p 119] (note the intensity scale difference between figures 9(b) and (c)) is the primary factor which is responsible for making blue the dominant colour of streamer coronas at lower extremities of sprites [1] and in blue jet type phenomena observed near thundercloud tops [5]. The red (1PN_2) emissions are not completely quenched at altitudes < 50 km and have been detected in red-filtered images of sprites [78]. A detailed calculation of the streamer colour requires knowledge of the spectral range of the colour TV system, the specifics of the observational geometry, allowing to account for the effects of the atmospheric transmission and factors such as the transmission through an aircraft window [72, 123]. Interested readers can find more discussion on related topics in section 4.2 in ([87] and references cited therein).

6.3. Comparison with selected laboratory experiments

The importance of the photoionization processes for the propagation of ionizing space-charge waves in gases had been recognized many decades ago ([124] and references cited therein).

Yi and Williams [125] have recently reported laboratory studies of positive and negative streamers in near atmospheric pressures N_2 and N_2/O_2 gas mixtures. The streamers were studied in a $\simeq 13$ cm gap with voltage rise times around 20 ns and typical streamer initiation times 30–50 ns. The typical electric fields used in experiments of Yi and Williams [125] were on the order of 10 kV cm^{-1} , which are a factor of four lower than those used in simulations reported in figure 8. However, some experiments were conducted at low pressures with the same applied voltages so effective fields in excess of $1.6E_k$ were considered [125, figure 10]. In this case streamers did exhibit propagation speeds exceeding 10^7 ms^{-1} in good agreement with overvolted streamers observed in sprites [8, 28, 120, 121] and with results on

streamer acceleration presented in [44]. A more frequent branching of positive streamers in comparison with negative ones was noted in both N_2 and N_2/O_2 mixtures. Streamers branched more frequently in N_2 and addition of small amounts of O_2 sharply reduced the branching. The addition of O_2 also increased the streamer propagation speed. All these effects were attributed by the authors to increase in the photoionization range, which is considerably longer for O_2 than N_2 [125]. These findings generally support the theoretical arguments discussed in [44]. In N_2 with 10% O_2 the measured diameters of positive (6 mm) and negative (8 mm) streamers are in good agreement with scaled diameters observed in sprites [16–18] (6 mm and 8 mm scale to ~ 90 m and 120 m, respectively, at 70 km altitude).

van Veldhuizen and Rutgers [122] have reported studies of positive streamers in air in a 2.5 cm gap with voltages up to 25 kV and voltage rise times less than 25 ns. Unique photographs of streamers with time exposures of only 0.8 ns were obtained. The work emphasized studies of streamer branching. The results indicate significant dependence of branching on electrode geometry, in particular, a factor of 10 increase in branching in a point-wire gap in comparison with a plane-protrusion gap. Also, it was established that enhanced branching in air occurs if a resistance is included in the pulse circuit [122, 126]. These findings indicate that branching is a complex phenomenon, which in real systems depends on a number of factors, in addition to the photoionization range and the electric field magnitude discussed in [44].

6.4. Emissions from streamers in weak uniform electric fields and comparison with recent satellite observations

It has been demonstrated in [44] (see also discussion related to figure 8 earlier in this paper) that the photoionization process is the most critical factor contributing to non-similar behaviour of streamers propagating in strong homogeneous external electric fields ($> E_k$, where E_k is the previously defined conventional breakdown threshold field). In this and the following subsections we present modelling results on the dynamics of streamers at various pressures developing in a point-to-plane discharge geometry [46], which are directly relevant to the interpretation of recent satellite-based observations of sprites [84–86] and recent laboratory experiments reported in [42, 43].

It is well known that a formed streamer can propagate in an electric field substantially lower than E_k ($E_k \simeq 32 \text{ kV cm}^{-1}$ at ground pressure and scales proportionally to neutral density at higher altitudes). Experimental and numerical simulation results have demonstrated that the minimum field required for the propagation of positive streamers in air at ground pressure stays close to the value 5 kV cm^{-1} ([113] and references therein). The existing sources about the similar field for the negative streamers indicate that this field is a factor of 2–3 higher than the corresponding field for the positive streamers [37, 113, p 361]. For the sprite phenomenon, the lightning-driven quasi-static electric field is smaller than E_k in the region below the sprite initiation altitude (see figure 3) and the streamers advancing in the weak electric fields ($E < E_k$) likely occupy a substantial part of the overall sprite volume and are responsible for most of the observed sprite emissions.

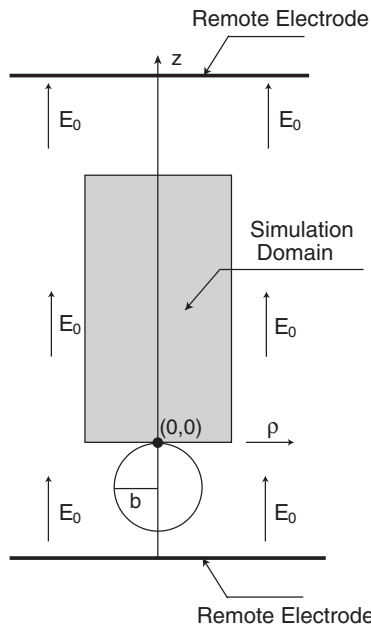


Figure 11. Simulation domain. A potential Φ_0 is applied to the conducting sphere with radius b which is put into an originally homogeneous field E_0 established by two remote plane electrodes [46, 62, 88, 113].

The studies of emissions of sprite streamers in weak fields are therefore important for correct interpretation of experimental data [62, 88].

In order to model the streamer propagation in both strong and weak electric fields, Liu and Pasko [46, 88] and Liu *et al* [62] adopted a simple setup proposed in [113] by introducing a small conducting sphere into a weak uniform electric field E_0 to strongly enhance the field around the sphere for initiation of streamers as shown in figure 11.

To conduct a direct comparison between the modelling results on emissions from sprite streamers and spectrophotometric measurements by the ISUAL instrument on the FORMOSAT-2 satellite, the modelling calculations for a sprite streamer propagating in a weak applied electric field ($E_0 = 5 N/N_0 \text{ kV cm}^{-1}$) at 70 km altitude reported in [88] (see figure 12) can be used. The modelled streamer is initiated in a high field region (the maximum field is $\sim 3E_k$, where $E_k \simeq 220 \text{ V m}^{-1}$ at 70 km), which is created by enhancement of the weak applied field around a small conducting sphere with a high potential. The streamer is then allowed to propagate into the weak field region. The longest propagation time of the simulated streamer is 0.53 ms, which is of the same order as the 1–2 ms lifetime of sprite streamer channel luminosity observed recently by a high-speed telescopic imaging system [20, 21].

The first four channels of ISUAL spectrophotometer are designed to measure LBH, 2PN_2 , 1NN_2^+ and 1PN_2 emissions, respectively. Channels 1 and 4 measure the broadband signal within the wavelength range 150–280 nm (LBH) and 609–753 nm (1PN_2), respectively [84]. Channels 2 and 3 measure the narrowband signal with centre wavelength at 337 (2PN_2) nm and 391.4 (1NN_2^+) nm, respectively [84]. The response curves of the photometer filters are given in [85]. The FUV emissions of the N_2 LBH band system suffer from attenuation when travelling through the atmosphere, and a

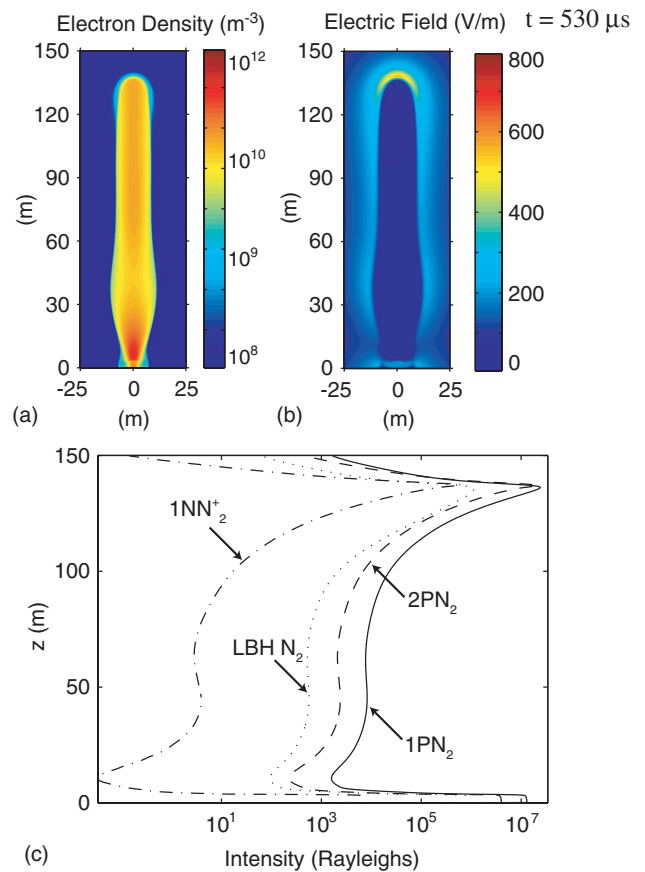


Figure 12. Modelling results on a streamer advancing in a weak electric field at 70 km altitude: (a) electron number density, (b) electric field and (c) intensity (in Rayleighs) profiles of 1PN_2 , 2PN_2 , 1NN_2^+ and LBH N_2 emissions along the central axis of the modelled streamer [62]. Reprinted with permission from the American Geophysical Union.

ground-based observer is not able to detect these emissions from sprites due to the strong attenuation by high density atmosphere at low altitudes. These effects appear to be important for satellite-based observations as well, and details of related calculations can be found in [62].

Figure 12(c) illustrates distributions of the intensities of optical emissions (in Rayleighs) associated with the model streamer shown in figure 12(a) [62]. The major difference between the optical emissions from the model streamers propagating in weak electric fields and those for the strong field cases reported in [44] and shown in figures 8–10 is the dark streamer channel. For a streamer developing in weak electric fields, the channel field (figure 12(b)) is very small and unable to effectively excite the electronic states of N_2 (figure 7), so that the emission intensities in the streamer channel are several orders of magnitude lower than those in the streamer head (figure 12(c)). Another important aspect is the enhancement of all the optical emissions in the streamer head (figure 12(c)). The mean energies of electrons in the streamer tip and the body are 9.3 eV and 1.8 eV, respectively [62]. The formation time of the model streamer is several hundreds of μs , which is much longer than the effective lifetimes of the upper states of all of the optical emission band systems considered (see table 1). The molecules excite, then radiate or degenerate due

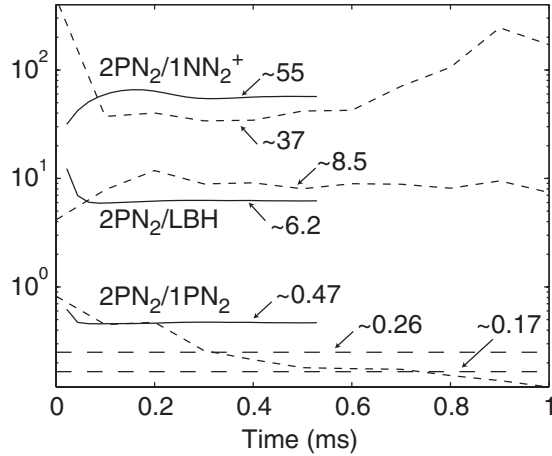


Figure 13. Intensity ratios calculated using modelling results for a streamer shown in figure 12 (solid line); intensity ratios from ISUAL measurements (dashed line) [62]. Reprinted with permission from the American Geophysical Union.

to quenching locally, and therefore the strong optical emissions are confined to the streamer head and do not spread along the streamer channel (see related discussion in section 3 of [44]). These results indicate that the observed streamer filaments in many cases may be produced by time averaging of optical luminosity coming from localized regions around streamer tips as streamers move through an observing instrument's field-of-view (FOV). Recent time-resolved (~ 1 ns) imaging of laboratory streamers in point-to-wire or point-to-plane discharge geometry conducted at ground and near ground pressures indicates that only the streamer heads are visible in the high time resolution pictures of streamers, and only the time-integrated pictures show luminous streamer filaments [41, 122, 125]. These results are also fully consistent with experiments discussed in [92, 100]. Although the quenching processes introduce non-similarities of the streamers and their optical emissions at different pressures [44], the modelling results presented in [62] and in figure 12 qualitatively agree with the above-cited experimental results at high pressures.

Figure 13 illustrates the intensity ratios of 2PN_2 to LBH , 1NN_2^+ and 1PN_2 obtained from the streamer modelling results and ISUAL spectrophotometric measurements [62]. The solid lines correspond to the streamer shown in figure 12. The dashed lines in figure 13 show the intensity ratios obtained by the ISUAL spectrophotometer with a time resolution of 0.1 ms. The three intensity ratios obtained from streamer modelling results and ISUAL spectrophotometric measurements reach the best agreement (within a factor of 2) at the initial development stage of sprites (within 1 ms after the sprite initiation) [62]. We note that the $2\text{PN}_2/\text{LBH}$ ratio is obtained from the streamer model assuming the source altitude 70 km. This ratio is expected to be higher for streamers developing at altitudes < 70 km due to quenching (see table 1 and discussion in [88]) and atmospheric attenuation effects on LBH emissions [62].

It is worthwhile to further discuss the ratio of 2PN_2 to 1NN_2^+ because of the large difference in their excitation energy thresholds (table 1). The fact that the ratio from ISUAL measurements is smaller than the ratio from the streamer modelling (see figure 13) implies that the maximum

electric field driving sprite emissions must be larger than $\sim 3E_k$ (the maximum field at the simulated streamer head shown in figure 12(b)). The weak applied field chosen for the streamer modelling in figure 12 is about one-sixth of the conventional breakdown threshold E_k at 70 km altitude. A slight increase in the magnitude of the applied field would lead to an increase in the electric field in the streamer head, leading to better agreement of streamer modelling and ISUAL measurements [62].

We note that the electric field magnitudes estimated in [62] and reviewed above ($\geq 3E_k$) are significantly greater than those obtained in [82] ($\sim E_k$), and the difference may be explained by the low temporal resolution of observations reported in [82], as discussed in [88]. Recently, Kuo *et al* [89] utilized the $2\text{PN}_2/1\text{NN}_2^+$ ratio to analyse five sprite events observed by the ISUAL instrument and estimated the upper limit of the electric field driving the sprite emissions to be greater than $3E_k$, in good agreement with the study reported in [62].

To summarize, we note that the direct comparison between ratios obtained from satellite data and from the streamer model reviewed above indicates that in order to explain the ISUAL spectrophotometric data the maximum field driving the emissions of an observed sprite event must be greater than three times the conventional breakdown threshold field. As concluded in [62], these findings are consistent with an assumption that most of the observed sprite emissions during initial sprite development originate from localized high field regions associated with tips of sprite streamers, in full agreement with the similar phenomenology of streamers documented in point-to-plane discharge geometry in laboratory experiments.

6.5. Similarity properties of streamers in weak uniform electric fields and comparison with recent laboratory experiments

The goal of this subsection is to illustrate photoionization effects on similarity properties of streamers developing at different pressures in air in point-to-plane discharge geometry, following the recently published work of Liu and Pasko [46].

Figure 14 shows results of model calculations corresponding to positive streamers developing at different pressures assuming $E_0 = 5N/N_0$ kV cm $^{-1}$ and $\Phi_0 = 9.5$ kV. We use the same approach for the presentation of results as was used in figure 8. To clearly demonstrate similarity properties of streamers at different pressures, the results presented in figures 14(b) and (c) are given at the moments of time, which are obtained by scaling ($\sim 1/N$) of the ground value, 10 ns, specified in figure 14(a). It follows from the results presented in figures 14(b)–(e) that streamers at 11 and 0.05 Torr pressures preserve similarity and propagate without branching, while a model streamer at 760 Torr (figure 14(a)) shows branching structures. The streamer at 760 Torr is narrower and its electron density is higher than the scaled streamers at low pressures (i.e. obtained by multiplication of their radius by N/N_0 and density by N_0^2/N^2). The results reported in [46] and reproduced in figure 14 agree with the conclusion drawn in [44] that the quenching of the excited singlet states of N_2 , emitting photoionizing radiation, is responsible for non-similar behaviour of streamers at high pressures (i.e. the streamer in

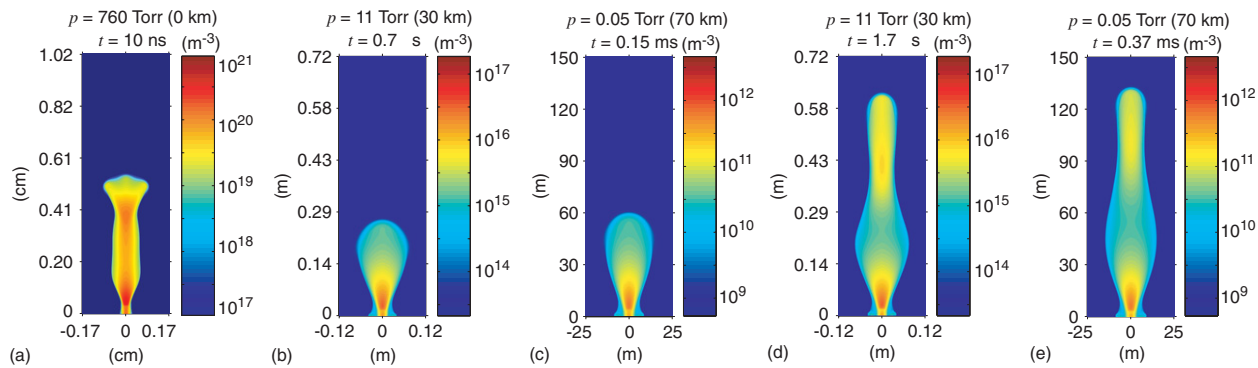


Figure 14. A cross-sectional view of the distribution of the electron number density for a positive streamer developing at different pressures in a field $E_0 = 5 N/N_0 \text{ kV cm}^{-1}$, and assuming spherical electrode potential $\Phi_0 = 9.5 \text{ kV}$. Panels (a), (b) and (c) correspond to streamers at moments of time $10 N_0/N \text{ ns}$. Panels (d) and (e) show fully developed streamers corresponding to panels (b) and (c), respectively. Reprinted from [46] with permission from the IOP Publishing Ltd.

figure 14(a)). The quenching altitude of the above-mentioned singlet states is $\sim 24 \text{ km}$ (corresponding to 30 Torr pressure). Therefore, the quenching effects are negligible at low pressures $p < 30 \text{ Torr}$ corresponding to altitudes $> 24 \text{ km}$, and streamers at 11 and 0.05 Torr pressures preserve similarity (figures 14(b) and (c)). At ground pressure, the excited singlet states are heavily quenched, and the photoionizing radiation level is reduced by a factor of ~ 20 in comparison with the cases of streamers at 11 and 0.05 Torr pressures (see [44] for additional discussion on related issues).

In [44], a physical mechanism has been proposed for streamer branching indicating that streamers are easier to branch at ground level due to the reduction in the pre-ionization level ahead of the streamer due to quenching of the N_2 states emitting photoionizing radiation. The results presented in figure 14 are consistent with this branching mechanism. A relationship has been proposed defining the streamer radius (r_{smax}) preceding the branching, $r_{\text{smax}} \simeq \kappa / \chi_{\text{min}} p_{\text{O}_2}$, where κ is a dimensionless parameter, χ_{min} is the absorption coefficient ($\text{cm}^{-1} \text{ Torr}^{-1}$) of O_2 at wavelength 102.5 nm and p_{O_2} is the partial pressure of O_2 [44]. It was suggested that the value of κ varies with pressure and that we generally expect lower values of κ and smaller splitting diameters of streamers at the ground level in comparison with sprite altitudes due to the quenching effects [44]. The results shown by figure 14 clearly verify this prediction.

We now discuss the modelling results from [46] presented in figure 14 in the context of recently published experimental work on the development of positive streamers at different pressures.

Results of experimental investigation of positive streamer discharges in air for the pressure range 760–300 Torr are reported in [42]. The streamers propagated in a gap with the same size $d = 30 \text{ mm}$ and were driven by the external electric field of the same magnitude $E_{\text{gap}} = 7 \text{ kV cm}^{-1}$ for all studied pressures. The streamers initiated from a needle anode and propagated towards a plane cathode. The time-integrated photographs clearly show that streamers exhibit many branches, several branches, and a single channel at pressures of 740 Torr, 500 Torr, and 380 Torr, respectively [42]. In terms of the discussion of similarity properties of streamers presented earlier in this review, the experimental setup used in [42] corresponds to a factor of two increase in the reduced

electric field E/N and a factor of two decrease in the effective gap size and radius of the anode (the effective gap size, for example, is defined as dN/N_0), when pressure is changed from 740 to 380 Torr. For accurate studies of the streamer similarity, however, it is desirable to keep the same reduced electric field and scale the gap and the point-electrode size as N_0/N (in other words, to keep the effective gap size dN/N_0 constant). In this particular experiment, therefore, factors which contribute to the observed non-similar behaviour of streamers at different pressures include (1) different reduced field magnitudes (2) different effective gap sizes and anode radii and (3) the pressure-defined quenching effects discussed earlier in this review. However, figure 3 in [42] demonstrates that the maximum diameter of the observed streamers does not scale as N_0/N , suggesting that κ varies with pressure and exhibits lower values at higher pressures. This finding is consistent with the behaviour predicted in [44] based on the fact that branching diameters of streamers are expected to increase with the reduction in pressure due to reduction in the quenching losses of excited N_2 molecules responsible for photoionizing radiation, as illustrated in [46] and figure 14. We emphasize, however, that different reduced electric fields, effective gap sizes and anode radii used in [42] do not allow direct quantitative verification of the quenching-based hypothesis advanced in [44].

Experimental studies of propagation and branching of positive streamers in air in a pressure range from 1010 to 100 mbar have been recently reported in [43]. The experiments were conducted in a 17 mm gap consisting of a point anode and a plane cathode, with adjustable anode voltage. The obtained time-integrated ($10 \mu\text{s}$) pictures of streamers demonstrate that streamer discharges have more and thinner channels at high pressures than at low pressures. By imaging streamers developing under conditions of different applied voltages (U) and pressures (p), the authors clearly established that streamer branching structures are not simply determined by U/p (or E/N). For the same values of U/p , streamers have more channels at high pressures than at low pressures. These findings are generally consistent with the modelling results presented in figure 14 and in [44] indicating that quenching effects facilitate easier branching of streamers at high pressures than at low pressures. We note, however, that following the same arguments as presented above with

relation to experiments in [42], the constant gap size and radius of point anode in experiments reported in [43] represent additional factors affecting the observed non-similar behaviour of streamers at different pressures (additional comments on this issue are provided in [46]).

In summary, the modelling results presented in [46] and briefly reviewed above emphasize that the quenching of singlet excited states of molecular nitrogen emitting photoionizing radiation is responsible for non-similar behaviour of streamers at pressures higher than approximately 30 Torr. The modelling results are consistent with recent experimental work showing that streamers have more and thinner channels and branch more frequently at higher (i.e. near atmospheric) pressures than at lower pressures [42, 43]. The results also demonstrate the importance of accounting for effects associated with electrode geometry for the interpretation of experimental studies on the similarity properties of streamers at various pressures.

7. Conclusions

In this paper we have presented a review of the general phenomenology and physical mechanism of sprites with primary emphasis on summarizing available experimental data on various emissions documented to date from sprites and interpretation of these data in the context of laboratory discharges and streamer models. We have also reviewed some of the recent results on modelling of streamers emphasizing the importance of the photoionization effects for understanding the observed morphological features of streamers at different pressures in air.

This review shows many important similarities between optical emissions associated with streamers documented in sprite discharges and emissions from pulsed corona discharges in laboratory experiments. The comparison of the laboratory and sprite discharges reveals the importance and need for further studies of processes related to the vibrational excitation of the ground state of N_2 molecules and pooling and resonant energy transfer reactions involving $N_2(A^3\Sigma_u^+)$ metastable species for the understanding of emissions originating from the $B^3\Pi_g$ and $C^3\Pi_u$ states of N_2 and NO γ -band emissions, during both initial and post-discharge stages of sprite discharge. We note that these problems, related to basic molecular physics of sprites, represent an important component of a broader range of other, currently unsolved, problems in sprite studies summarized recently in [45], which include, in particular, studies of streamer-to-spark transition in sprites and relationship of sprites and high air pressure leader processes, initiation and propagation of sprite streamers in low applied electric fields, branching of sprite streamers and effects related to the thermal runaway electron phenomenon in streamer tips in sprites.

Acknowledgments

This research was supported by NSF ATM-0134838 grant to Penn State University. The author would like to thank Santolo De Benedictis and members of the International Scientific Committee of the 18th European Conference on the Atomic and Molecular Physics of Ionized Gases for the invitation to write this review paper and to present a related talk at

the conference. He would also like to thank Steve Cummer, Elizabeth Kendall (nee Gerken) and Walt Lyons for providing electronic copies of their figures for inclusion in this review.

References

- [1] Sentman D D, Wescott E M, Osborne D L, Hampton D L and Heavner M J 1995 Preliminary results from the Sprites94 campaign: red sprites *Geophys. Res. Lett.* **22** 1205–8
- [2] Neubert T 2003 On sprites and their exotic kin *Science* **300** 747–9
- [3] Lyons W A 2006 The meteorology of transient luminous events—an introduction and overview *Sprites, Elves and Intense Lightning Discharges (NATO Science Series II: Mathematics, Physics and Chemistry vol 225)* ed M Füllekrug *et al* (Heidelberg: Springer) pp 19–56
- [4] Franz R C, Nemzek R J and Winckler J R 1990 Television image of a large upward electric discharge above a thunderstorm system *Science* **249** 48
- [5] Wescott E M, Sentman D, Osborne D, Hampton D and Heavner M 1995 Preliminary results from the Sprites94 aircraft campaign: 2 Blue jets *Geophys. Res. Lett.* **22** 1209–12
- [6] Lyons W A, Nelson T E, Armstrong R A, Pasko V P and Stanley M A 2003 Upward electrical discharges from thunderstorm tops *Bull. Am. Meteorol. Soc.* **84** 445–54
- [7] Lyons W A 1996 Sprite observations above the U.S. high plains in relation to their parent thunderstorm systems *J. Geophys. Res.* **101** 29641
- [8] Stanley M, Krehbiel P, Brook M, Moore C, Rison W and Abrahams B 1999 High speed video of initial sprite development *Geophys. Res. Lett.* **26** 3201–4
- [9] Fukunishi H, Takahashi Y, Kubota M, Sakanoi K, Inan U S and Lyons W A 1996 Elves: Lightning-induced transient luminous events in the lower ionosphere *Geophys. Res. Lett.* **23** 2157–60
- [10] Inan U S, Barrington-Leigh C, Hansen S, Glukhov V S, Bell T F and Rairden R 1997 Rapid lateral expansion of optical luminosity in lightning-induced ionospheric flashes referred to as ‘elves’ *Geophys. Res. Lett.* **24** 583–6
- [11] Pasko V P, Stanley M A, Mathews J D, Inan U S and Wood T G 2002 Electrical discharge from a thundercloud top to the lower ionosphere *Nature* **416** 152–4
- [12] Su H T, Hsu R R, Chen A B, Wang Y C, Hsiao W S, Lai W C, Lee L C, Sato M and Fukunishi H 2003 Gigantic jets between a thundercloud and the ionosphere *Nature* **423** 974–6
- [13] Pasko V P 2003 Electric jets *Nature* **423** 927–9
- [14] Füllekrug M, Mareev E A and Rycroft M J 2006 *Sprites, Elves and Intense Lightning Discharges (NATO Science Series II: Mathematics, Physics and Chemistry vol 225)* (Heidelberg: Springer)
- [15] Boccippio D J, Williams E R, Heckman S J, Lyons W A, Baker I T and Boldi R 1995 Sprites, ELF transients, and positive ground strokes *Science* **269** 1088–91
- [16] Gerken E A, Inan U S and Barrington-Leigh C P 2000 Telescopic imaging of sprites *Geophys. Res. Lett.* **27** 2637–40
- [17] Gerken E A and Inan U S 2002 A survey of streamer and diffuse glow dynamics observed in sprites using telescopic imagery *J. Geophys. Res.* **107** 1344
- [18] Gerken E A and Inan U S 2003 Observations of decameter-scale morphologies in sprites *J. Atmos. Solar Terr. Phys.* **65** 567–72
- [19] Gerken E A and Inan U S 2005 Streamers and diffuse glow observed in upper atmospheric electrical discharges *IEEE Trans. Plasma Sci.* **33** 282–3
- [20] Marshall R A and Inan U S 2005 High-speed telescopic imaging of sprites *Geophys. Res. Lett.* **32** L05804

- [21] Marshall R A and Inan U S 2006 High-speed measurements of small-scale features in sprites: sizes and lifetimes *Radio Science* **41** RS6S43
- [22] Stenbaek-Nielsen H C, Moudry D R, Wescott E M, Sentman D D and Sao Sabbas F T 2000 Sprites and possible mesospheric effects *Geophys. Res. Lett.* **27** 3829–32
- [23] Pasko V P and Stenbaek-Nielsen H C 2002 Diffuse and streamer regions of sprites *Geophys. Res. Lett.* **29** 1440
- [24] Barrington-Leigh C P, Inan U S and Stanley M 2001 Identification of sprites and elves with intensified video and broadband array photometry *J. Geophys. Res.* **106** 1741–50
- [25] Wescott E M, Stenbaek-Nielsen H C, Sentman D D, Heavner M J, Moudry D R and Sabbas F T S 2001 Triangulation of sprites, associated halos and their possible relation to causative lightning and micrometeors *J. Geophys. Res.* **106** 10467–77
- [26] Miyasato R, Taylor M J, Fukunishi H and Stenbaek-Nielsen H C 2002 Statistical characteristics of sprite halo events using coincident photometric and imaging data *Geophys. Res. Lett.* **29** 2033
- [27] Miyasato R, Fukunishi H, Takahashi Y and Taylor M J 2003 Energy estimation of electrons producing sprite halos using array photometer data *J. Atmos. Solar Terr. Phys.* **65** 573–81
- [28] Moudry D R, Stenbaek-Nielsen H C, Sentman D D and Wescott E M 2003 Imaging of elves, halos and sprite initiation at 1 ms time resolution *J. Atmos. Solar Terr. Phys.* **65** 509–18
- [29] Moore R C, Barrington-Leigh C P, Inan U S and Bell T F 2003 Early/fast VLF events produced by electron density changes associated with sprite halos *J. Geophys. Res.* **108** 1363
- [30] Cummer S A, Jaughey N C, Li J B, Lyons W A, Nelson T E and Gerken E A 2006 Submillisecond imaging of sprite development and structure *Geophys. Res. Lett.* **33** L04104
- [31] McHarg M G, Kammae T and Stenbaek-Nielsen H C 2005 Streamer formation in sprites *EOS Trans. Am. Geophys. Union* **86** (52) (Fall Meet. Suppl. Abstract AE11A-04)
- [32] McHarg M G, Stenbaek-Nielsen H C and Kammae T 2007 Streamer development in sprites *Geophys. Res. Lett.* **34** (in review)
- [33] Pasko V P, Inan U S and Bell T F 1998 Spatial structure of sprites *Geophys. Res. Lett.* **25** 2123–6
- [34] Raizer Y P, Milikh G M, Shneider M N and Novakovski S V 1998 Long streamers in the upper atmosphere above thundercloud *J. Phys. D: Appl. Phys.* **31** 3255–64
- [35] Petrov N I and Petrova G N 1999 Physical mechanisms for the development of lightning discharges between a thundercloud and the ionosphere. *Tech. Phys.* **44** 472–5
- [36] Pasko V P, Inan U S and Bell T F 2001 Mesosphere-troposphere coupling due to sprites *Geophys. Res. Lett.* **28** 3821–4
- [37] Raizer Y P 1991 *Gas Discharge Physics* (New York: Springer)
- [38] van Veldhuizen E M (ed) *Electrical Discharges for Environmental Purposes: Fundamentals and applications* (New York: Nova Science)
- [39] Tardiveau P, Marode E, Agneray A and Cheaib M 2001 Pressure effects on the development of an electric discharge in non-uniform fields *J. Phys. D: Appl. Phys.* **34** 1690–6
- [40] Tardiveau P and Marode E 2003 Point-to-plane discharge dynamics in the presence of dielectric droplets *J. Phys. D: Appl. Phys.* **36** 1204–11
- [41] Ebert U, Montijn C, Briels T M P, Hundsdorfer W, Meulenbroek B, Rocco A and van Veldhuizen E M 2006 The multiscale nature of streamers. *Plasma Sources Sci. Technol.* **15** S118–29
- [42] Pancheshnyi S V, Nudnova M and Starikovskii A Y 2005 Development of a cathode-directed streamer discharge in air at different pressures: experiment and comparison with direct numerical simulation. *Phys. Rev. E* **71** 016407
- [43] Briels T M P, van Veldhuizen E M and Ebert U 2005 Branching of positive discharge streamers in air at varying pressures *IEEE Trans. Plasma Sci.* **33** 264–5
- [44] Liu N and Pasko V P 2004 Effects of photoionization on propagation and branching of positive and negative streamers in sprites *J. Geophys. Res.* **109** A04301
- [45] Pasko V P 2006 Theoretical modeling of sprites and jets *Sprites, Elves and Intense Lightning Discharges* (NATO Science Series II: Mathematics, Physics and Chemistry vol 225) ed M Füllekrug *et al* (Heidelberg: Springer) pp 253–93
- [46] Liu N and Pasko V P 2006 Effects of photoionization on similarity properties of streamers at various pressures in air *J. Phys. D: Appl. Phys.* **39** 327–34
- [47] Wilson C T R 1925 The electric field of a thundercloud and some of its effects *Proc. Phys. Soc. London* **37** 32D
- [48] Pasko V P, Inan U S, Bell T F and Taranenko Y N 1997 Sprites produced by quasi-electrostatic heating and ionization in the lower ionosphere *J. Geophys. Res.* **102** 4529–61
- [49] Boeuf J P 2003 Plasma display panels: physics, recent developments and key issues *J. Phys. D: Appl. Phys.* **36** R53–79
- [50] Pasko V P, Inan U S and Bell T F 1999 Mesospheric electric field transients due to tropospheric lightning discharges *Geophys. Res. Lett.* **26** 1247–50
- [51] Marshall T C and Rust W D 1993 Two types of vertical electrical structures in stratiform precipitation regions of mesoscale convective systems *Bull. Am. Meteorol. Soc.* **74** 2159
- [52] Shepherd T R, Rust W D and Marshall T C 1996 Electric fields and charges near 0°C in stratiform clouds. *Mon. Weather Rev.* **124** 919–38
- [53] Lyons W A, Nelson T E, Williams E R, Cummer S A and Stanley M A 2003 Characteristics of sprite-producing positive cloud-to-ground lightning during the 19 July 2000 STEPS mesoscale convective systems *Mon. Weather Rev.* **131** 2417–27
- [54] Cummer S A, Inan U S, Bell T F and Barrington-Leigh C P 1998 ELF radiation produced by electrical currents in sprites *Geophys. Res. Lett.* **25** 1281
- [55] Hu W Y, Cummer S A and Lyons W A 2002 Lightning charge moment changes for the initiation of sprites *Geophys. Res. Lett.* **29** 1279
- [56] Cummer S A 2003 Current moment in sprite-producing lightning *J. Atmos. Solar Terr. Phys.* **65** 499–508
- [57] Cummer S A and Lyons W A 2005 Implication of lightning charge moment changes for sprite initiation *J. Geophys. Res.* **110** A04304
- [58] Cummer S A, Frey H U, Mende S B, Hsu R R, Su H T, Chen A B, Fukunishi H and Takahashi Y 2006 Simultaneous radio and satellite optical measurements of high-altitude sprite current and lightning continuing current *J. Geophys. Res.* **111** A10315
- [59] Zabolotin N A and Wright J W 2001 Role of meteoric dust in sprite formation *Geophys. Res. Lett.* **28** 2593–6
- [60] van der Velde O A, Mika A, Soula S, Haldoupis C, Neubert T and Inan U S 2006 Observations of the relationship between sprite morphology and in-cloud lightning processes *J. Geophys. Res.* **111** D15203
- [61] Adachi T, Fukunishi H, Takahashi Y, Hiraki Y, Hsu R R, Su H T, Chen A B, Mende S B, Frey H U and Lee L C 2006 Electric field transition between the diffuse and streamer regions of sprites estimated from ISUAL/array photometer measurements *Geophys. Res. Lett.* **33** L17803
- [62] Liu N, Pasko V P, Burkhardt D H, Frey H U, Mende S B, Su H T, Chen A B, Hsu R R, Lee L C, Fukunishi H and Takahashi Y 2006 Comparison of results from sprite streamer modeling with spectrophotometric measurements by ISUAL instrument on FORMOSAT-2 satellite *Geophys. Res. Lett.* **33** L01101
- [63] Mende S B, Rairden R L, Swenson G R and Lyons W A 1995 Sprite spectra: N₂ 1 PG band identification *Geophys. Res. Lett.* **22** 2633–7

- [64] Hampton D L, Heavner M J, Wescott E M and Sentman D D 1996 Optical spectral characteristics of sprites *Geophys. Res. Lett.* **23** 89–93
- [65] Green B D, Fraser M E, Rawlins W T, Jeong L, Blumberg W A M, Mende S B, Swenson G R, Hampton D L, Wescott E M and Sentman D D 1996 Molecular excitation in Sprites *Geophys. Res. Lett.* **23** 2161–4
- [66] Bucselo E, Morrill J, Heavner M, Siefiring C, Berg S, Hampton D, Moudry D, Wescott E and Sentman D 2003 $N_2(B^3\Pi_g)$ and $N_2^+(A^2\Pi_u)$ vibrational distributions observed in sprites *J. Atmos. Solar Terr. Phys.* **65** 583–90
- [67] Liszka L 2004 On the possible infrasound generation by sprites *J. Low Freq. Noise, Vibration and Active Cont.* **23** 85–93
- [68] Farges T, Blanc E, Le A Pichon, Neubert T and Allin T H 2005 Identification of infrasound produced by sprites during the Sprite2003 campaign *Geophys. Res. Lett.* **32** L01813
- [69] Liszka L and Hobaru Y 2006 Sprite-attributed infrasonic chirps - their detection, occurrence and properties between 1994 and 2004 *J. Atmos. Solar-Terr. Phys.* **68** 1179–88
- [70] Phillips D M 1976 Determination of gas temperature from unresolved bands in spectrum from a nitrogen discharge *J. Phys. D: Appl. Phys.* **9** 507–21
- [71] Vallance-Jones A V 1974 *Aurora* (Norwell, MA) Reidel
- [72] Morrill J S, Bucselo E J, Pasko V P, Berg S L, Benesch W M, Wescott E M and Heavner M J 1998 Time resolved N_2 triplet state vibrational populations and emissions associated with red sprites *J. Atmos. Solar Terr. Phys.* **60** 811–29
- [73] Kammae T, Stenbaek-Nielsen H C and McHarg M G Sprite spectra at high time resolution *Poster Session Booklet 2006 CEDAR Workshop (Santa Fe, NM, USA, 19–23 June 2006)* p 19
- [74] Kammae T, Stenbaek-Nielsen H C and McHarg M G 2007 Altitude resolved sprite spectra with 3 ms temporal resolution *Geophys. Res. Lett.* **34** (in review)
- [75] Lowke J J 1992 Theory of electrical breakdown in air—the role of metastable oxygen molecules *J. Phys. D: Appl. Phys.* **25** 202–10
- [76] Naidis G V 1999 Simulation of streamer-to-spark transition in short non-uniform air gaps *J. Phys. D: Appl. Phys.* **32** 2649–54
- [77] Kamaratos E 2006 Active nitrogen and oxygen: Enhanced emissions and chemical reactions *Chem. Phys.* **323** 271–94
- [78] Armstrong R A, Shorter J A, Taylor M J, Suszcynsky D M, Lyons W A and Jeong L S 1998 Photometric measurements in the SPRITES' 95 and 96 campaigns of nitrogen second positive (399.8 nm) and first negative (427.8 nm) emission *J. Atmos. Solar Terr. Phys.* **60** 787–99
- [79] Armstrong R A, Suszcynsky D M, Lyons W A and Nelson T E 2000 Multi-color photometric measurements of ionization and energies in sprites *Geophys. Res. Lett.* **27** 653–7
- [80] Suszcynsky D M, Roussel R-Dupre, Lyons W A and Armstrong R A 1998 Blue-light imagery and photometry of sprites *J. Atmos. Solar Terr. Phys.* **60** 801–9
- [81] Takahashi Y, Fujito M, Watanabe Y, Fukunishi H and Lyons W A 2000 Temporal and spatial variations in the intensity ratio of N_2 1st and 2nd positive bands in SPRITES *Middle Atmosphere and Lower Thermosphere Electrodynamics Advances in Space Research* **26** 1205–8
- [82] Morrill J, Bucselo E, Siefiring C, Heavner M, Berg S, Moudry D, Slinker S, Fernsler R, Wescott E, Sentman D and Osborne D 2002 Electron energy and electric field estimates in sprites derived from ionized and neutral N_2 emissions *Geophys. Res. Lett.* **29** 1462
- [83] Chern J L, Hsu R R, Su H T, Mende S B, Fukunishi H, Takahashi Y and Lee L C 2003 Global survey of upper atmospheric transient luminous events on the ROCSAT-2 satellite *J. Atmos. Solar Terr. Phys.* **65** 647–59
- [84] Mende S B, Frey H U, Hsu R R, Su H T, Chen A B, Lee L C, Sentman D D, Takahashi Y and Fukunishi H 2005 D region ionization by lightning-induced EMP *J. Geophys. Res.* **110** A11312
- [85] Mende S B, Chang Y S, Chen A B, Frey H U, Fukunishi H, Geller S P, Harris S, Heeterdks H, Hsu R R, Lee L C, Su H T and Takahashi Y 2006 Spacecraft based studies of transient luminous events *Sprites, Elves and Intense Lightning Discharges (NATO Science Series II: Mathematics, Physics and Chemistry vol 225)* (Heidelberg: Springer) pp 123–49
- [86] Frey H U, Mende S B, Cummer S A, Chen A B, Hsu R R, Su H T, Chang Y S, Adachi T, Fukunishi H and Takahashi Y 2005 Beta-type stepped leader of elve-producing lightning *Geophys. Res. Lett.* **32** L13824
- [87] Pasko V P and George J J 2002 Three-dimensional modeling of blue jets and blue starters *J. Geophys. Res.* **107** 1458
- [88] Liu N and Pasko V P 2005 Molecular nitrogen LBH band system far-UV emissions of sprite streamers *Geophys. Res. Lett.* **32** L05104
- [89] Kuo C L, Hsu R R, Su H T, Chen A B, Lee L C, Mende S B, Frey H U, Fukunishi H and Takahashi Y 2005 Electric fields and electron energies inferred from the ISUAL recorded sprites *Geophys. Res. Lett.* **32** L19103
- [90] Moss G D, Pasko V P, Liu N and Veronis G 2006 Monte Carlo model for analysis of thermal runaway electrons in streamer tips in transient luminous events and streamer zones of lightning leaders *J. Geophys. Res.* **111** A02307
- [91] Gallimberti I, Hepworth J K and Klewe R C 1974 Spectroscopic investigation of impulse corona discharges *J. Phys. D: Appl. Phys.* **7** 880–99
- [92] Simek M, Babicky V, Clupek M, DeBenedictis S, Dilecce G and Sunka P 1998 Excitation of $N_2(C^3\Pi_u)$ and $NO(A^2\Sigma^+)$ states in a pulsed positive corona discharge in N_2 , N_2-O_2 and N_2-NO mixtures *J. Phys. D: Appl. Phys.* **35** 591–602
- [93] Simek M 2002 The modelling of streamer-induced emission in atmospheric pressure, pulsed positive corona discharge: N_2 second positive and $NO-\gamma$ systems *J. Phys. D: Appl. Phys.* **35** 1967–80
- [94] Teich T H 1993 Emission spectroscopy of corona discharges *Non-Thermal Plasma Techniques for Pollution Control, NATO ASI Ser. vol G34 (part A)* ed B M Penetrante and S E Schultheis (Berlin: Springer) pp 231–48
- [95] Matveev A A and Silakov V P 1998 Method of calculation of specific radiant emittance of the bands of 1^- and 2^+ systems of nitrogen in the non-equilibrium nitrogen-oxygen plasma *Physics and Technology of Electric Power Transmission* vol Book 1 ed A F Djakov (Moscow: MPEI Publishers) pp 201–18
- [96] Djakov A F, Bobrov Y K, Bobrova L N and Yuorguelenas Y V 1998 Streamer discharge plasma parameters determination in air on a base of a measurement of radiation of the molecular bands of nitrogen *Physics and Technology of Electric Power Transmission* vol Book 1 ed A F Djakov (Moscow: MPEI Publishers) pp 219–233
- [97] Kim Y, Hong S H, Cha N S, Song Y H and Kim S J 2003 Measurements of electron energy by emission spectroscopy in pulsed corona and dielectric barrier discharges *J. Adv. Oxidation Technol.* **6** 17–22
- [98] Kozlov K V, Wagner H E, Brandenburg R and Michel P 2001 Spatio-temporally resolved spectroscopic diagnostics of the barrier discharge in air at atmospheric pressure *J. Phys. D: Appl. Phys.* **34** 3164–76
- [99] Kozlov K V, Brandenburg R, Wagner H E, Morozov A M and Michel P 2005 Investigation of the filamentary and diffuse mode of barrier discharges in N_2/O_2 mixtures at atmospheric pressure by cross-correlation spectroscopy *J. Phys. D: Appl. Phys.* **38** 518–29
- [100] Simek M, DeBenedictis S, Dilecce G, Babicky V, Clupek M and Sunka P 2002 Time and space resolved analysis of $N_2(C^3\Pi_u)$ vibrational distributions in pulsed positive corona discharge *J. Phys. D: Appl. Phys.* **35** 1981–90
- [101] Tochikubo F and Teich T H 2000 Optical emission from a pulsed corona discharge and its associated reactions *Japan. J. Appl. Phys.* **39** 1343–50
- [102] Ono R and Oda T 2005 Spatial distribution of ozone density in pulsed corona discharges observed by two-dimensional

- laser absorption method *J. Phys. D: Appl. Phys.* **37** 730–5
- [103] Kennealy J P, Del Greco F P, Caledonia G E and Green B D Nitric oxide chemiexcitation occurring in the reaction between metastable nitrogen atoms and oxygen molecules *J. Chem. Phys.* **69** 1574–84
- [104] Bailey S M, Barth C A and Solomon S C 2002 A model of nitric oxide in the lower thermosphere *J. Geophys. Res.* **107** 1205
- [105] Zhao G B, Garikipati S V B, Hu X, Argyle M D and Radosz M 2005 Effect of oxygen on nonthermal plasma reactions of nitrogen oxides in nitrogen *AIChE J.* **51** 1800–12
- [106] Simek M, Clupek M, Babicky V and Sunka P 2006 Production of reactive species by atmospheric pressure streamers in N₂-O₂ mixtures *Pure Appl. Chem.* **78** 1213–25
- [107] DeBenedictis S, Dilecce G and Simek M 1997 The NO(A²Σ⁺) excitation mechanism in a N₂-O₂ pulsed RF discharge. *J. Phys. D: Appl. Phys.* **30** 2887–94
- [108] Dhali S K and Williams P F 1987 Two-dimensional studies of streamers in gases *J. Appl. Phys.* **62** 4696–707
- [109] Vitello P A, Penetrante B M and Bardsley J N 1994 Simulation of negative-streamer dynamics in nitrogen *Phys. Rev. E* **49** 5574–98
- [110] Rocco A, Ebert U and Hundsdorfer W 2002 Branching of negative streamers in free flight *Phys. Rev. E* **66** 035102
- [111] Roth R J 1995 *Industrial Plasma Engineering, Vol. 1: Principles* (Bristol: IOP Publishing)
- [112] Achat S, Teisseyre Y and Marode E 1992 The scaling of the streamer-to-arc transition in a positive point-to-plane gap with pressure *J. Phys. D: Appl. Phys.* **25** 661–8
- [113] Babaeva N Y and Naidis G V 1997 Dynamics of positive and negative streamers in air in weak uniform electric fields *IEEE Trans. Plasma Sci.* **25** 375–9
- [114] Kulikovskiy A A 2000 The role of photoionization in positive streamer dynamics *J. Phys. D: Appl. Phys.* **33** 1514–24
- [115] Pancheshnyi S V, Starikovskaia S M and Starikovskii A Y 2001 Role of photoionization processes in propagation of cathode-directed streamer *J. Phys. D: Appl. Phys.* **34** 105–15
- [116] Zheleznyak M B, Mnatsakanyan Kh A and Sizykh S V 1982 Photoionization of nitrogen and oxygen mixtures by radiation from a gas discharge *High Temp.* **20** 357–62
- [117] Pancheshnyi S V 2005 Role of electronegative gas admixtures in streamer start, propagation and branching phenomena *Plasma Sources Sci. Technol.* **14** 645–53
- [118] Naidis G V 2006 On photoionization produced by discharges in air *Plasma Sources Sci. Technol.* **15** 253–55
- [119] Segur P, Bourdon A, Marode E, Bessieres D and Paillot J H 2006 The use of an improved eddington approximation to facilitate the calculation of photoionization in streamer discharges *Plasma Sources Sci. Technol.* **15** 648–60
- [120] Moudry D R, Stenbaek-Nielsen H C, Sentman D D and Wescott E M 2002 Velocities of sprite tendrils *Geophys. Res. Lett.* **29** 1992
- [121] McHarg M G, Haaland R K, Moudry D R and Stenbaek-Nielsen H C 2002 Altitude-time development of sprites *J. Geophys. Res.* **107** 1364
- [122] van Veldhuizen E M and Rutgers W R 2002 Pulsed positive corona streamer propagation and branching *J. Phys. D: Appl. Phys.* **35** 2169–79
- [123] Wescott E M, Sentman D D, Heavner M J, Hampton D L and Vaughan O H Jr 1998 Blue jets: their relationship to lightning and very large hailfall and their physical mechanisms for their production *J. Atmos. Solar Terr. Phys.* **60** 713–24
- [124] Winn W P 1967 Ionizing space-charge waves in gases *J. Appl. Phys.* **38** 783–90
- [125] Yi W J and Williams P F 2002 Experimental study of streamer in pure N₂ and N₂/O₂ mixtures and a ≈13 cm gap *J. Phys. D: Appl. Phys.* **35** 205–18
- [126] van Veldhuizen E M, Kemps P C M and Rutgers W R 2002 Streamer branching in a short gap: the influence of the power supply *IEEE Trans. Plasma Sci.* **30** 162–3